



Process optimisation for n-type Bi₂Te₃ films electrodeposited on flexible recycled carbon fibre using response surface methodology

Priyanka R. Jagadish¹, Mohammad Khalid^{2,*} , Nowshad Amin⁴, Lau Phei Li¹, and Andy Chan³

¹ Department of Chemical & Environmental Engineering, Faculty of Engineering, The University of Nottingham Malaysia Campus, 43500 Semenyih, Selangor, Malaysia

² Research Centre for Nano-Materials and Energy Technology, Sunway University, No. 5, Jalan Universiti, 47500 Bandar Sunway, Selangor Darul Ehsan, Malaysia

³ Department of Civil Engineering, Faculty of Engineering, The University of Nottingham Malaysia Campus, 43500 Semenyih, Selangor, Malaysia

⁴ Solar Energy Research Institute, National University of Malaysia, 43600 Bangi, Selangor, Malaysia

Received: 25 March 2017

Accepted: 9 June 2017

Published online:

20 June 2017

© Springer Science+Business Media, LLC 2017

ABSTRACT

Electrodeposition method was used to synthesise n-type bismuth telluride (Bi₂Te₃) films on recycled carbon fibre under different deposition conditions. D-optimal model under response surface methodology was used to design the experiment and optimise the following deposition parameters: deposition potential (*V*), deposition time (*h*), deposition temperature (°C) and electrolyte composition (molar concentration). The effects of electrodeposition parameters were evaluated within the limits of deposition potential (−0.10 to −0.60 V), deposition time (0.5–3 h), deposition temperature (25–60 °C) and electrolyte composition (0.2, 0.4 and 0.6 of Bi/(Bi + Te)). The optimum conditions for the electrodeposition parameters with the least amount of chemicals, time and energy consumption were −0.10 V, 0.5 h, 25 °C and 0.240 Bi/(Bi + Te), respectively, for deposition potential, deposition time, deposition temperature and electrolyte composition. Moreover, the validation of predicted values shows good agreement with experimental results with 1.45% deviation.

Introduction

Thermoelectric modules are defined as devices that generate an electric potential gradient from a thermal gradient, or vice versa, without any actuating parts. The conventional and commercial thermoelectric power generators consist of a rigid ceramic substrate that acts

as the sink plate and absorber plate with thermoelectric elements stacked in the middle [1]. However, the lack of flexibility and the sheer size of these conventional devices have proven to be the Achilles Heel, thus limiting its potential applications. Hence, in order to enhance thermal contact with heat sources of different geometry and prevent large thermal energy losses [2],

Address correspondence to E-mail: khalids@sunway.edu.my

there is a need for a thermoelectric generator (TEG) that easily conforms to any surface [3].

Flexible TEGs have been fabricated in the past using inorganic materials such as Bi_2Te_3 and Sb_2Te_3 on flexible substrates [2–4] or by using flexible polymeric materials such as poly(3,4-ethylenedioxythiophene) (PEDOT) [5, 6] and polydimethyl siloxane (PDMS) [7]. However, polymeric-based thermoelectric materials have relatively lower ZT values (0.3–0.4) approximately three orders lower than that of inorganic materials. On the other hand, Bi_2Te_3 has the highest reported value of $ZT \approx 1.4$ at a room temperature range of 200–400 K which is suitable for portable power generators [3, 8, 9]. The cost of a TEG can be reduced by employing recycled materials as flexible substrate; one such suitable candidate is recycled carbon fibre (RCF).

RCF has been primarily explored for its mechanical properties in structural applications [10–12]; however, recycling leads to a slight decrease in tensile strength properties which makes it challenging to be used for structural purposes currently. Though recycling leads to reduction of mechanical properties, the electrically conductive nature of carbon fibres is preserved despite recycling [13]. The high electrical conductivity of carbon fibre sheets (10^4 – 10^{-5} Sm^{-1}), has enabled it to be integrated into polymer matrix composites and also cement composites for thermoelectric and heating applications as fillers [14–16]. Thus, due to its inherent electrical conductive nature RCF has the potential to be used as a thermoelectric substrate.

Thus, in this study RCF is chosen as a viable substrate to replace the conventional ceramics due to its flexible, lightweight nature and as a means to close the recycling loop for RCF.

The primary parameter that determines the optimal performance of a thermoelectric module is the figure of merit (ZT) given by Eq. (1).

$$ZT = \frac{T\alpha^2}{\rho\kappa} \quad (1)$$

where α is the Seebeck coefficient ($\mu\text{V}/\text{K}$); T is the temperature (K); ρ is the electrical resistivity ($\Omega \text{ m}$); and κ is the thermal conductivity (W/mK). Seebeck coefficient is given the primary attention in this study due to its significant contribution to the ZT value as shown in Eq. (1).

In this study, the thermoelectric element chosen to be deposited on RCF is n-type bismuth telluride (Bi_2Te_3) as it has the highest reported value of $ZT \approx 1.4$ at a room temperature range of 200–400 K

which is suitable for portable power generators [3, 8, 9]. Electrodeposition was chosen to deposit Bi_2Te_3 on RCF as it is a cost-effective, room temperature operation and provides a large area for deposition which is suitable for industrial application, and the composition of the films can be easily monitored by altering the electrodeposition parameters [17]. Though electrodeposition of Bi_2Te_3 using nitric acid electrolytes has been widely studied from the year 1993 [18], a majority of work focused on varying deposition potentials with different substrates [17, 19–22]. There was also some work done by varying the amount of bismuth and tellurium precursors to observe its effects on thermoelectric properties [23–25]. Both parameters showed substantial effects on thermoelectric properties; however, those are not the only parameters that affect electrodeposition. Faraday's law has also identified deposition time as a crucial parameter that affects the amount of semiconductor deposited [26] on a substrate that have yet to be investigated in any study pertaining Bi_2Te_3 . Electrolyte bath temperature is also another vital parameter in electrodeposition which was thought to improve electrochemical kinetics and led to grain size increment [27, 28]. However, the effects of parameters such as deposition time and deposition temperature have yet to be investigated for the electrodeposition of Bi_2Te_3 .

The novelty of this study is the usage of the design of experiments (DOE) to study the combined effect of experimental parameters such as deposition potential, electrolyte composition, deposition time and deposition temperature on the Seebeck coefficient of Bi_2Te_3 , which have yet to be reported in the literature thus far. Most researches pertaining electrodeposition of Bi_2Te_3 have been studied by varying one deposition parameter at a time while maintaining the others. This univariate approach may not result in optimum experimental conditions that will yield the highest properties due to the neglected experimental domain. However, with the multivariate approach using DOE, this study will be able to explore a larger experimental domain thus resulting in higher optimum values.

A D-optimal model under response surface methodology (RSM) was used to study the inter-parameter interactions, leading to the subsequent optimisation of parameters that yield the optimum Seebeck coefficient of Bi_2Te_3 . The D-optimal approach was preferred in this case compared to

that of central composite design (CCD), Box–Behnken method and factorial method as it yielded the least amount of experimental runs but with comprehensive information on each parameter and its subsequent effect on Seebeck coefficient [29, 30]. D-optimal has a flexible design structure that allows the researcher to vary numeric factors either in discrete or in continuous manners, which is not plausible with other rigid designs such as CCD, Box–Behnken that vary parameters based on fixed levels. This study ultimately aims to determine the combination of experimental parameters that will yield the optimum Seebeck coefficient with the least amount of chemicals and energy. In addition to that, the data obtained in this study will be compared to that of author's previous work [31] to highlight the improvement brought about by DOE on the Seebeck coefficient due to the multivariate approach employed.

Materials and methods

The methodology discussed in this section has been adapted from author's previous work [31].

Carbon Fibres

The carbon fibres used in this experiment are recycled Toray T600 carbon fibre recovered via fluidised bed process by Recycled Carbon Fibre Limited (RCF) Coseley, UK.

Preparation of Electrolyte

The Bi₂Te₃ films were deposited from electrolyte solutions consisting of 1 M of 65% aqueous nitric acid bath with three different compositions of Bi(NO₃)₃·5H₂O (>98%, Sigma-Aldrich) and TeO₂ (>98%, Sigma-Aldrich) as shown in Table 1.

Table 1 Different compositions of bismuth and tellurium ions in electrolyte

Electrolyte composition in molar concentration ratio (Bi/(Bi + Te))	Concentration of Bi and Te ions (mM)	
	Bi(NO ₃) ₃ ·5H ₂ O (mM)	TeO ₂ (mM)
0.20	2.5	10
0.40	6.7	10
0.60	15	10

Electrochemical Deposition

Electrodeposition was carried out using a potentiostat (VersaStat-3, Princeton Applied Research) at varying deposition temperature from 25 to 60 °C. The potentiostat was used with a standard three-cell electrode configuration whereby the working electrode is the virgin/recycled carbon fibre sheet with dimension of 8 cm × 0.5 cm, the reference electrode is a silver/silver chloride (Ag/AgCl) in 1 M of potassium chloride (KCl), and the counter electrode is a platinum rod. The schematic for the electrodeposition setup is depicted in Fig. 1. Potentiostatic mode was used for varying deposition time from 0.5 to 3 h and varying deposition potential from −0.10 to −0.60 V.

Measurement of Seebeck Coefficient

The Seebeck coefficient is calculated using the formula:

$$\alpha = \frac{\Delta V}{\Delta T} = \frac{V_H - V_C}{T_H - T_C} \quad (2)$$

whereby α is the combined measured value of the Seebeck coefficient of copper (α_{Cu}) and carbon fibre (α_{CF}); therefore, the Seebeck coefficient of carbon fibre is given by Eq. (3). ΔV in millivolts is the potential difference generated between V_H , the potential at the hot side and V_C , the potential at cold side, ΔT in Kelvin is the temperature induced between the T_H , temperature on the hot side and T_C , temperature on the cold side.

$$\alpha_{CF} = \alpha_{Cu} - \alpha \quad (3)$$

The Seebeck coefficient was measured using an inhouse measurement system as shown in Fig. 2. The Seebeck coefficients of the carbon fibres were calculated using Eq. (3) by taking an average of all six readings.

Figure 1 Schematic of a three-cell electrode setup.

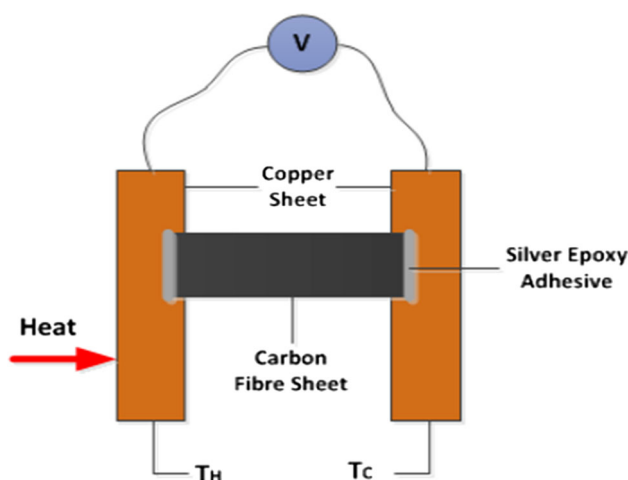
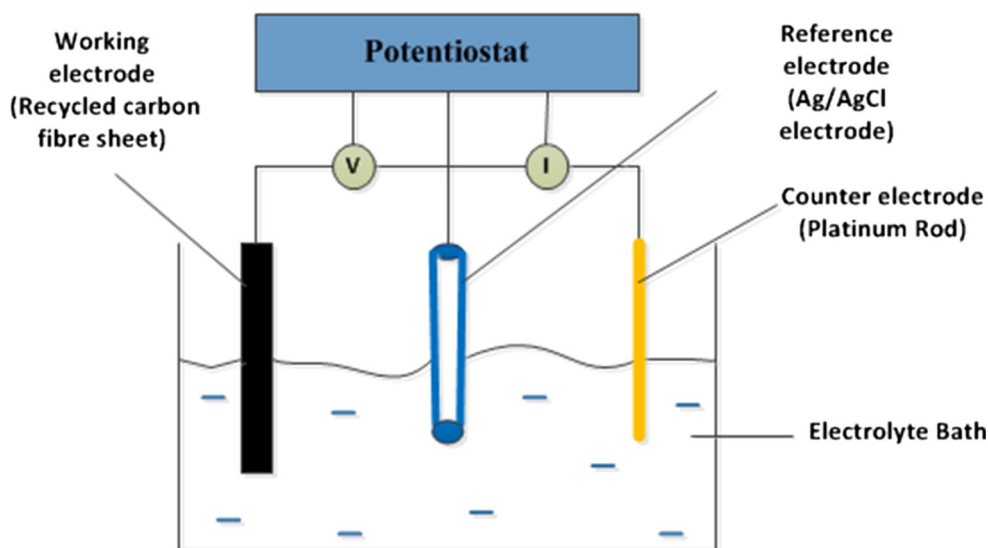


Figure 2 Schematic setup for Seebeck coefficient measurement [31].

Field emission scanning electron microscope (FESEM) and energy-dispersive X-ray (EDX) analysis

The carbon fibre sheets are cut into $1\text{ cm} \times 1\text{ cm}$ and placed onto a double-sided sticky tape that was positioned on sample pins before being placed into the FESEM machine. The FESEM images were taken using the FEI Quanta 400 to obtain the morphological structure of the bismuth telluride deposition. No further sample preparation was required at this stage as carbon fibres are naturally conductive. The EDX analysis was carried out to determine the percentage distribution of bismuth and tellurium in the deposition.

Experimental design and statistical analysis

Response surface methodology (RSM) was used to design the sets of experiments for this study. In RSM, the primary objective is to optimise a response that is influenced by various experimental parameters and also helps to quantify the relationship between a response and the vital experimental parameters [32]. The D-optimal model under RSM was used to investigate the effects of four different experimental parameters in electrodeposition of Bi_2Te_3 on one response output (i.e. Seebeck coefficient) based on 23 sets of experiments. The four experimental parameters were deposition potential (A), deposition time (B), deposition temperature (C) and electrolyte composition, $\text{Bi}/(\text{Bi} + \text{Te})$ (D). Parameters A , B and C are numeric continuous-type factors varied over two levels (low and high), while parameter D was numeric discrete-type factor varied over three levels as shown in Table 2.

The experimental parameters were varied based on previous studies. The deposition potentials were varied from -0.60 to -0.10 V, as [19] mentioned that all potentials more negative than 0.50 V were suitable for the deposition of Bi_2Te_3 . Martin-Gonzalez et al. [19] observed that potentials between -0.10 and -0.20 V led to stoichiometric Bi_2Te_3 ; however, a close to stoichiometric Bi_2Te_3 was also observed close to -0.50 V. Many studies [22, 33, 34] have concluded that -0.10 to -0.20 V is ideal for the stoichiometric deposition of Bi_2Te_3 . A stoichiometric Bi_2Te_3 is often associated with better thermoelectric properties [31, 35, 36]. Thus, in this study the effect of deposition

Table 2 Parameter ranges chosen for experimental study using D-optimal

Coded name	Variable name	Type	Parameter range		Parameter unit
A	Deposition potential	Continuous	Level 1/low	−0.6	V
			Level 2/high	−0.1	
B	Deposition time	Continuous	Level 1/low	0.5	Hours
			Level 2/high	3	
C	Deposition temperature	Continuous	Level 1/low	25	°C
			Level 2/high	60	
D	Electrolyte composition	Discrete	Level 1	0.2	mM
			Level 2	0.4	
			Level 3	0.6	

Table 3 D-optimal experimental design along with experimental and predicted Seebeck coefficient

Run	A Deposition potential (V)	B Deposition time (hours)	C Deposition temperature (°C)	D Bi/(Bi + Te)	Seebeck coefficient (μV/K)		Percentage difference between experimental and predicted (%)
					Experimental	Predicted	
1	−0.60	0.5	43.6	0.2	−10.48	−10.40	0.76
2	−0.10	2.7	25.0	0.6	−12.55	−12.65	0.79
3	−0.10	0.6	60.0	0.2	−10.32	−11.18	8.33
4	−0.60	0.5	43.6	0.2	−9.55	−10.40	8.90
5	−0.42	3.0	41.7	0.6	−14.05	−14.78	4.94
6	−0.10	0.6	60.0	0.2	−12.04	−11.18	7.14
7	−0.60	0.5	25.0	0.6	−10.79	−10.49	2.78
8	−0.35	1.6	29.0	0.6	−10.77	−10.46	2.88
9	−0.60	3.0	60.0	0.2	−11.82	−11.94	1.02
10	−0.36	1.7	51.3	0.2	−11.19	−10.72	4.20
12	−0.41	0.5	60.0	0.4	−12.22	−11.68	4.40
13	−0.60	1.7	60.0	0.6	−12.07	−11.63	3.65
14	−0.10	3.0	25.0	0.2	−10.80	−10.69	1.02
15	−0.10	0.5	25.0	0.6	−10.66	−11.05	3.66
16	−0.10	0.5	25.0	0.2	−13.52	−13.05	3.50
17	−0.60	1.7	60.0	0.6	−11.14	−11.63	4.40
18	−0.10	0.5	56.5	0.6	−10.97	−11.18	1.91
19	−0.10	1.8	43.4	0.4	−14.60	−15.08	3.29
20	−0.60	3.0	25.0	0.4	−10.66	−10.72	0.56
21	−0.43	1.8	25.0	0.2	−9.29	−9.48	2.05
22	−0.10	3.0	53.0	0.2	−16.06	−16.03	0.19

potential on the Seebeck coefficient of Bi₂Te₃ will be studied and verified using D-optimal model. The effect of deposition time on Seebeck coefficient of Bi₂Te₃ has not been reported in the literature thus far as most studies were carried out for a fixed duration of an hour, and in this study the effect of electrodeposition duration on Seebeck coefficient of Bi₂Te₃ will be clearly demonstrated. In addition to time, temperature is also another parameter that has not been investigated despite bath temperature playing a vital role in electrochemical kinetics [27]. Thus, the bath temperature in this study will be carried out up to

60 °C, due to the limitation of the Ag/AgCl electrode that is only able to withstand a maximum temperature of 75 °C. Electrolyte composition and its effect on the stoichiometric compositions of Bi₂Te₃ were also studied by Kim and Oh [24], and in this study the ideal electrolyte composition that leads to the best Seebeck coefficient will be determined.

The response output for the D-optimal RSM design is the Seebeck coefficient measured. The four experimental parameters and the response output are fitted together in a reduced quadratic polynomial model as shown in Eq. (4):

Table 4 Analysis of variance (ANOVA) for electrodeposition parameters of Bi₂Te₃ on RCF

Source	Sum of squares	Degree of freedom df	Mean square	F value	p value	Significance
Model	66.75	11	6.07	11.43	0.0003 ^a	Significant
A—deposition potential	27.86	1	27.86	52.45	<0.0001 ^a	Significant
B—deposition time	27.38	1	27.38	51.55	<0.0001 ^a	Significant
C—deposition temperature	17.66	1	17.66	33.26	0.0002 ^a	Significant
D-Bi/(Bi + Te)	8.32	1	8.32	15.67	0.0027 ^a	Significant
AB	5.47	1	5.47	10.31	0.0093 ^a	Significant
AC	2.11	1	2.11	3.97	0.0744 ^b	Insignificant
BC	27.03	1	27.03	50.90	<0.0001 ^a	Significant
BD	14.90	1	14.90	28.05	0.0003 ^a	Significant
CD	2.80	1	2.80	5.28	0.0444 ^a	Significant
B ²	4.08	1	4.08	7.68	0.0198 ^a	Significant
D ²	9.55	1	9.55	17.99	0.0017 ^a	Significant
Residual	5.31	10	0.53			
Lack of fit	1.70	6	0.28	0.32	0.8996 ^b	Insignificant
Pure error	3.61	4	0.90			
Cor total	72.06	21				
SD	0.73	R ²	0.9263			
Mean	-11.87	Adj R ²	0.8452			
Coefficient of variation (CV %)	6.14	Pred R ²	0.6823			
Predicted residual sum of squares (PRESS)	22.89	Adeq Precision	12.155			

^a Significant at “p value” less than 0.05

^b Insignificant at “p value” more than 0.05

$$Y = B_0 + \sum B_i X_i + \sum B_{ij} X_i X_j + \sum B_{ii} X_i^2 \quad (4)$$

where Y is the response output, B_0 is independent constant effect, B_i is the linear/individual effect, X_i are the independent experimental parameters ($i = A, B, C, D$), B_{ij} is the interaction effect ($i = A, B, C, D$ and $j = A, B, C, D$), and B_{ii} is the squared effect.

The data collected were analysed using multiple regressions to fit the quadratic model through analysis of variance (ANOVA) to study the significance of each experimental parameter and their interactions during the electrodeposition of Bi₂Te₃ on RCF. The response surface models developed were then optimised to determine the required conditions for energy efficient deposition of Bi₂Te₃ on RCF.

Results and discussions

Model fitting and analysis of variance (ANOVA)

The design of experiments generated by D-optimal RSM design with varying electrodeposition conditions

along with the experimental and predicted values of Seebeck coefficient is shown in Table 3.

The experimental outcome of the D-optimal design above is fitted to a quadratic polynomial equation as shown in Eq. (5)

$$Y = -13.33 - 1.50A - 1.44B - 1.21C - 0.71D - 0.72AB - 0.49AC - 2.16BC - 1.18BD - 0.53CD - 1.05B^2 + 2.13D^2 \quad (5)$$

where Y is the Seebeck coefficient ($\mu\text{V}/\text{K}$); A, B, C and D are deposition potential, deposition time, deposition temperature and electrolyte composition, respectively.

The F value and p value in the analysis of variance (ANOVA) determine the significance of the model, model parameters and model parameter interactions. p values smaller than 0.05 indicate that the model terms are significant thus greatly contributing to the Seebeck coefficient [37]. The F and p values obtained in this study are shown in Table 4.

Thus, from the table above all parameters $A, B, C, D, AB, BC, BD, CD, B^2$ and D^2 have significant effect on the Seebeck coefficient as they have a p value less

Figure 3 Normal probability plot of residuals.

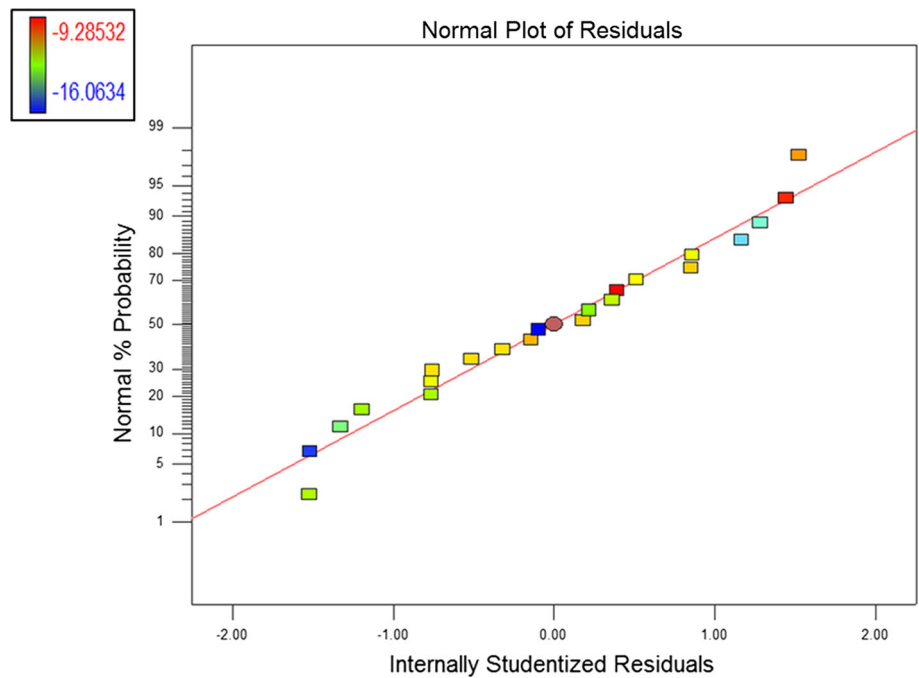
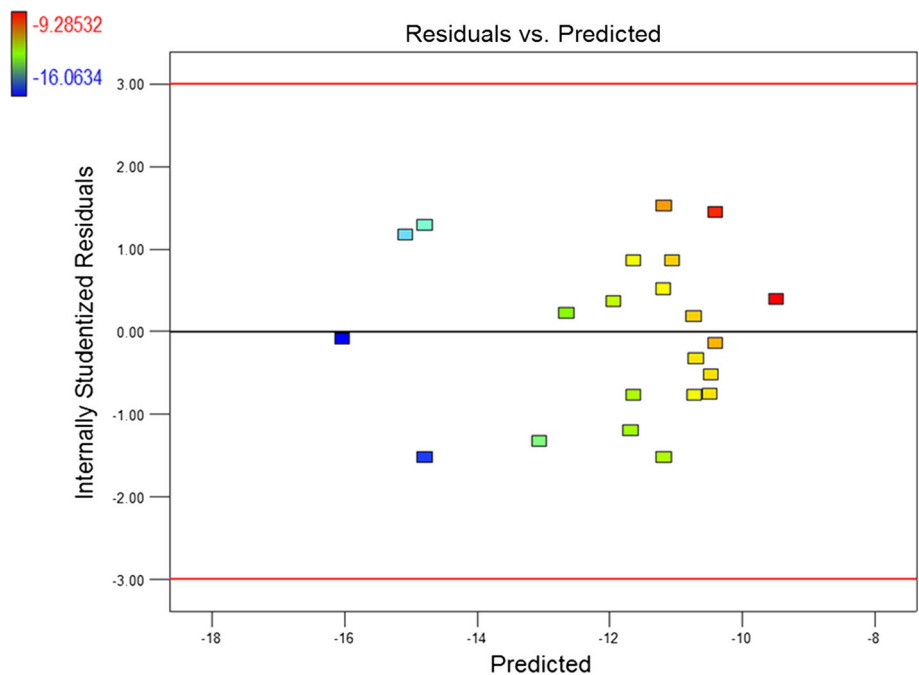


Figure 4 Plot of residuals versus predicted.

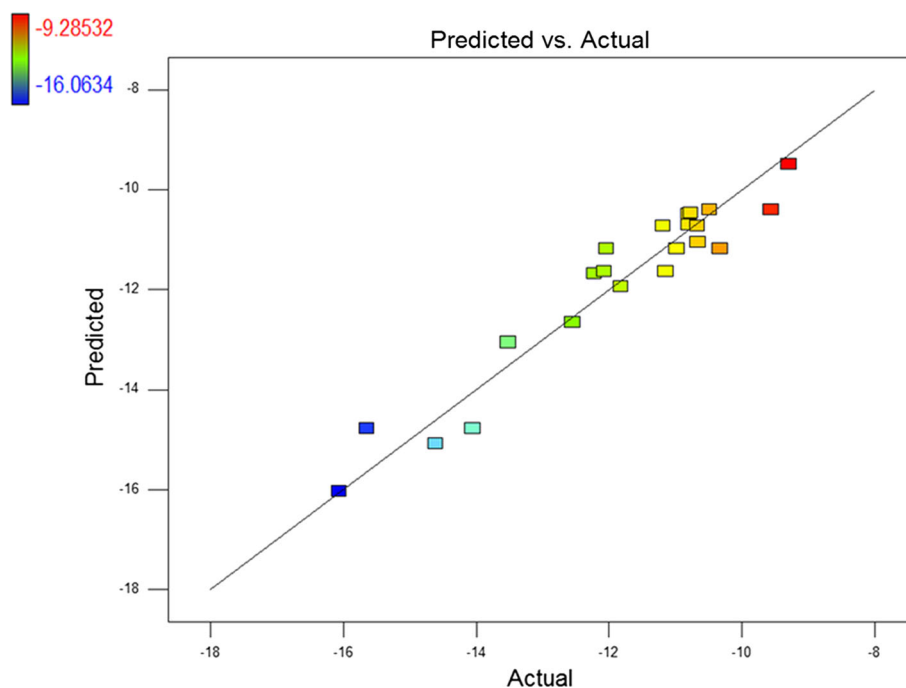


than 0.05 which indicates 95% of confidence. The model is significant which is also complemented with the high non-significance of the lack of fit approximately 90%. This ensures that the D-optimal quadratic model fits the experimental data well, thus

giving a better robustness to the design for predicting the response of electrodeposited samples.

The determination coefficient (R^2) for Seebeck coefficient of 92.63% implies that the variations could be explained well by the fitted model. The adjusted

Figure 5 Predicted against actual values of Seebeck coefficient.



and predicted R^2 is also in reasonable agreement with difference less than 0.2, ensuring the model provides good predictions for the outcomes.

The model was further confirmed with the normal probability plot as shown in Fig. 3. The data form an approximate straight line on a normal probability plot that ensures no abnormality in data population. It is observed in Fig. 4 that the practical results are distributed randomly within the range of internally studentized residuals of ± 3.00 that confirms the 95% confidence limit, implying that the fitted model is appropriate and the availability of variance assumption.

Figure 5 presents the comparison between the predicted and experimental measured Seebeck coefficient, which shows that they are in good agreement.

Screening of parameters and response surface analysis

The interaction between electrodeposition parameters and the Seebeck coefficient of Bi_2Te_3 -coated recycled carbon fibres was investigated by 3D response surface plots. Based on the formulated quadratic model (Eq. 5), the response surface plots for the interaction effects of deposition time, deposition potential, deposition temperature, electrolyte composition and their interactions are depicted in Figs. 6, 7, 8, 9 and 10, respectively.

The interaction between deposition potential and deposition time, and their combined effect on Seebeck coefficient are shown in Fig. 6. It is clear from Fig. 6 that longer deposition time and lower deposition potential individually lead to higher Seebeck coefficient. The highest Seebeck coefficient of $-18.03 \mu\text{V}/\text{K}$ is obtained at a deposition potential of -0.10 V and 3-h deposition time. A similar deposition potential for the reduction in bismuth and tellurium ions was observed by [17, 18] at -0.062 V which is close to the observed potential in this study using DOE. Martín-González et al. [19] also discovered that stoichiometric Bi_2Te_3 was deposited at potentials close to -0.12 V , and this could have resulted in the high Seebeck coefficient that was observed in this study. Magri et al. [20] discovered that deposition time affects the Bi_2Te_3 film thickness, concluding that electrical resistivity decreases and the mobility of electrons improves with prolonging deposition time. Thus, it is justified in this study that the Seebeck coefficient improves linearly with deposition time.

Figure 7 illustrates the combined effect of deposition temperature and deposition time on Seebeck coefficient. It is observed that higher deposition temperature and longer deposition time lead to a higher Seebeck coefficient. It was observed that a sample deposited at 60°C and 0.6 h has 59 wt% of Te and 39 wt% of Bi leading to stoichiometric Bi_2Te_3 ,

Figure 6 3D response surface plot illustrating the effect of deposition potential and deposition time.

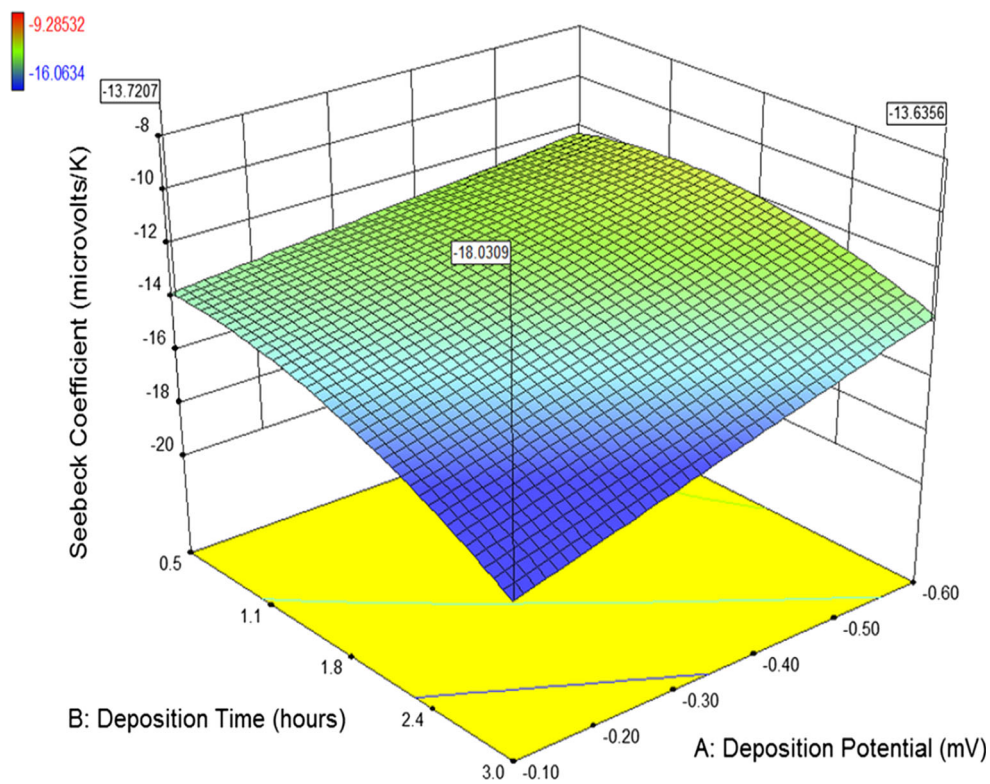
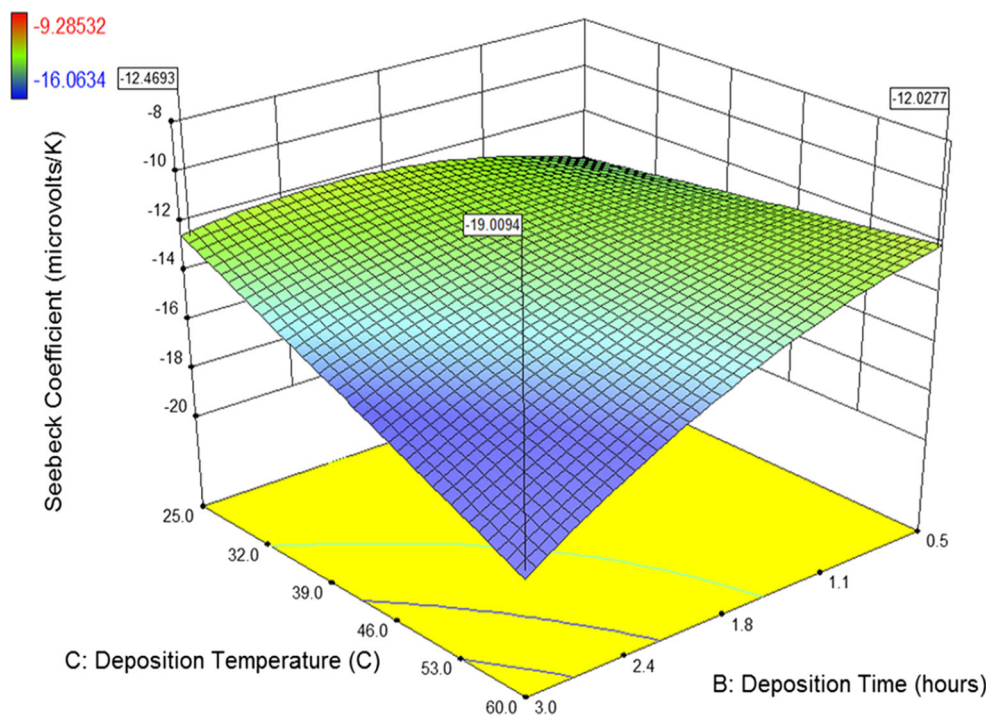


Figure 7 3D response surface plot illustrating the effect of deposition temperature and deposition time.



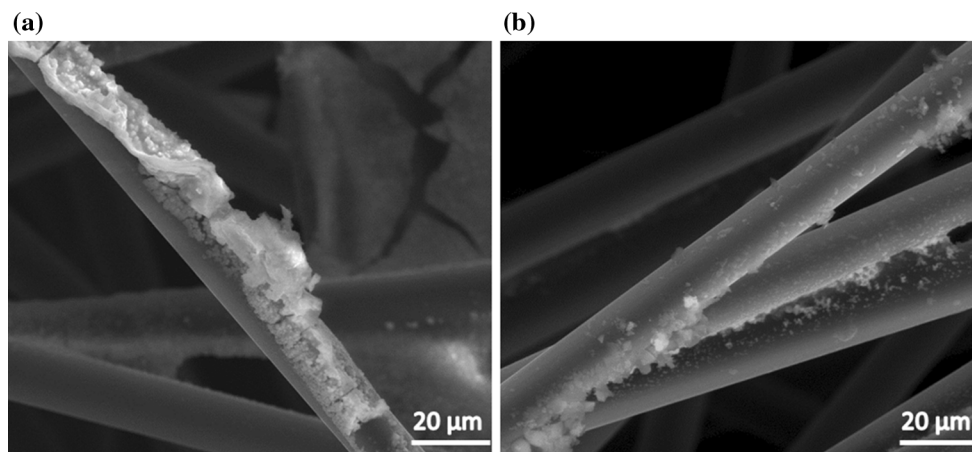
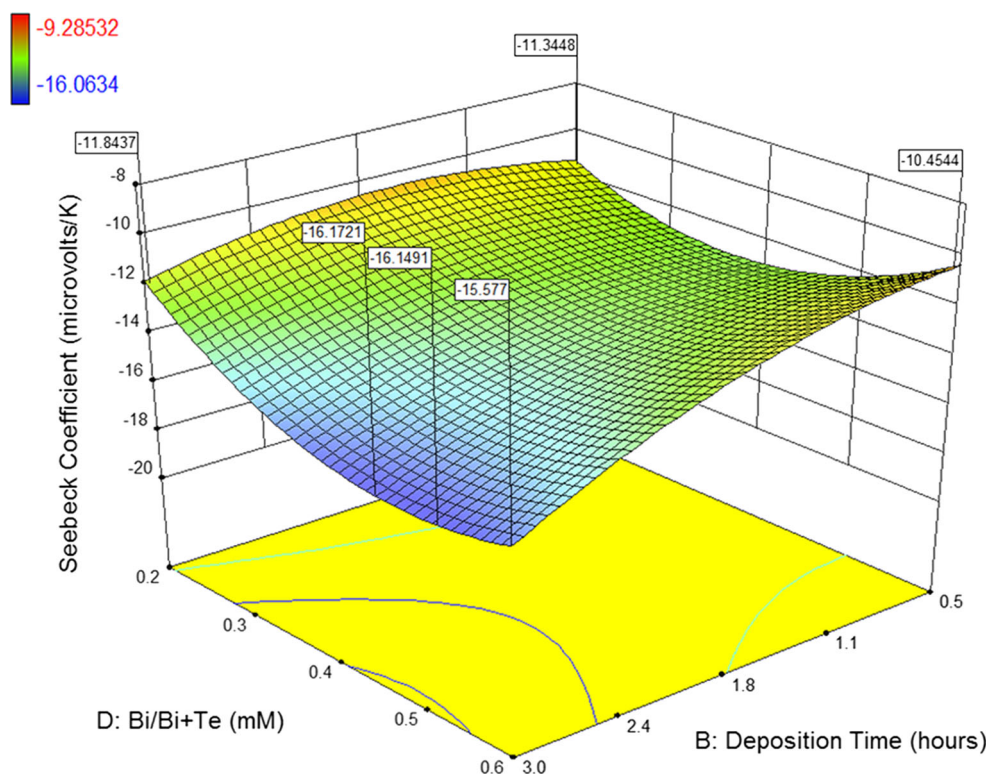


Figure 8 Surface morphologies of Bi_2Te_3 -coated RCF **a** at 60 °C and 0.60 h, **b** at 25 °C and 0.50 h both carried out at -0.10 V and 0.2 Bi/(Bi + Te).

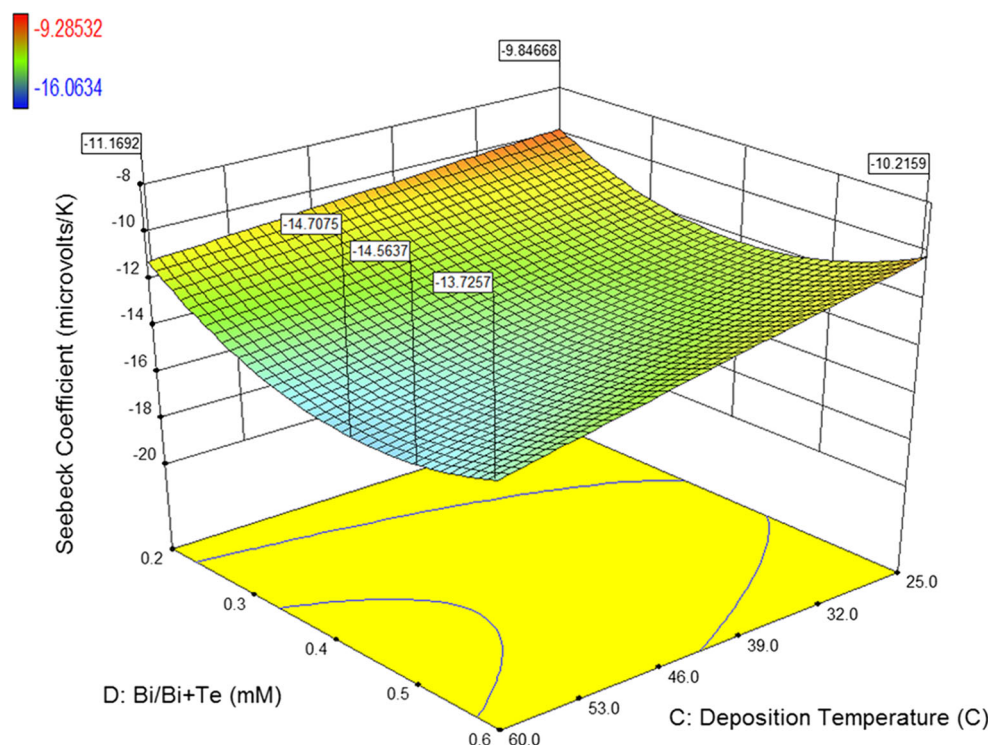
Figure 9 3D response surface plot illustrating the effect of electrolyte composition and deposition time.



whereas another sample deposited at 25 °C and 0.5 h has 80 wt% of Te and 20 wt% of Bi that is far from stoichiometric composition. The difference in the atomic percentage could be attributed to the change in surface adsorption temperature as the electrolyte temperature increases, thus allowing a redistribution of atoms attributed to the temperature rise. In

addition to that, Bi_2Te_3 coats RCF better at higher temperatures than at lower temperatures owing to the increase in grain size that results from higher electrolyte temperature as shown in Fig. 8. A similar relationship between electrolyte temperature and amount of coating on substrate was observed by [38, 39].

Figure 10 3D response surface plot illustrating the effect of electrolyte composition and deposition temperature.



The combined effect of electrolyte composition and deposition time on Seebeck coefficient is shown in Fig. 9. The ideal electrolyte composition for the highest Seebeck coefficient $-16.14 \mu\text{V}/\text{K}$ is between 0.4 and 0.5 ratio of Bi/(Bi + Te). This could essentially be attributed because stoichiometric Bi_2Te_3 , yields a 0.4 ratio. A longer deposition time yields a higher Seebeck coefficient, and the observed trend may be due to time-dependent mass transfer between Bi^{3+} and HTeO^{2+} ions with the working electrode [40].

There is also a clear correlation between deposition temperature and electrolyte composition on Seebeck coefficient as shown in Fig. 10. There is a linear relationship between deposition temperature and Seebeck coefficient, whereas Seebeck coefficient increases with electrolyte composition until a ratio of 0.4 then it begins to deteriorate. The highest Seebeck coefficient of $-14.71 \mu\text{V}/\text{K}$ is achievable at 60°C and 0.4 Bi/(Bi + Te) electrolyte ratio.

Optimisation and validation of the RSM-derived predictive model

In this study, the best Seebeck coefficient of Bi_2Te_3 -coated RCF obtained is $-17.249 \mu\text{V}/\text{K}$ with the following parameters as shown in Table 5.

The Seebeck value obtained through the design of experiments (DOE) in this study has shown a 33% improvement as compared to our previous study ($-12.99 \mu\text{V}/\text{K}$) of electrochemically deposited Bi_2Te_3 on RCF [31]. This drastic improvement in Seebeck coefficient may have arisen due to the multiparameter interaction that was studied in this work. Conventionally, most research pertaining electrodeposition of Bi_2Te_3 has been studied using the univariate approach in which most of the deposition parameters are maintained at constant values while one parameter is varied in the chosen pattern. However, the optimum conditions studied previously are only determined by varying one parameter at a time that may not accurately represent the real time process as it neglects the possibility of parameter interaction that is highly likely. In addition to that, the univariate approach may result in optimum conditions that are dependent on a particular starting condition and may not represent a whole experimental domain leaving some parts unanalysed due to the univariate approach.

This is clearly proven in our studies that a multivariate approach brings about an improvement in the properties due to the larger domain investigated, we are able to identify interactions between deposition parameters thus resulting in property enhancement

as compared to a univariate approach. Besides that, by using a multivariate approach with DOE, we are able to investigate a large pool of experimental parameters based on only 23 experimental runs, whereas the same in univariate approach may have resulted in a large number of experimental runs.

The results discussed above suggest that a higher Seebeck coefficient is attainable at longer deposition time, higher deposition temperature and moderate amount of Bi and Te precursors. However, the increase in value of these parameters results in a

Table 5 Parameters yielding the highest Seebeck coefficient for Bi₂Te₃-coated RCF

Deposition potential (V)	−0.175
Deposition time (h)	2.22
Deposition temperature (°C)	57.54
Electrolyte composition (Bi/(Bi + Te))	0.395

Table 6 Comparison of Seebeck coefficient and experimental conditions between work done with DOE and without DOE

	Bi ₂ Te ₃ - coated RCF (without DOE) [31]	Bi ₂ Te ₃ - coated RCF (with DOE)
Seebeck coefficient (μV/K)	−12.99	−13.42
Deposition potential (V)	−0.50	−0.10
Deposition time (h)	1	0.50
Deposition temperature (°C)	25	25
Electrolyte composition (Bi/(Bi + Te))	0.444	0.240

longer and more expensive deposition system that may not be economically feasible for industrial purposes. Thus, this study attempts to find the optimum Seebeck coefficient by minimising deposition time, temperature and the amount of precursor chemicals used in the electrolyte. This was aided by the desirability function in Design Expert 9 software so that the optimum Seebeck coefficient at low deposition temperature, short deposition time and least expensive electrolyte composition could be determined. The analysis suggested that a combination of 0.5 h of deposition time, 25 °C deposition temperature, 0.240 Bi/(Bi + Te) electrolyte composition and −0.10 V of deposition potential had a high desirability of 0.871. This combination of parameters was expected to yield a −13.62 μV/K Seebeck coefficient of Bi₂Te₃-coated RCF.

An experiment to replicate the obtained optimum conditions was carried out to validate the predicted response. The experimental result obtained was −13.42 μV/K, which is in close agreement with the predicted value above with only 1.45% difference.

Performance of Bi₂Te₃-coated RCF under optimum conditions

In this section, the performance of Bi₂Te₃-coated RCF (using DOE) obtained in this study was compared to the author's previous work [31] on Bi₂Te₃-coated RCF (without using DOE). The Seebeck coefficient of Bi₂Te₃-coated RCF (with DOE) was 3.3% higher than the Seebeck coefficient reported without DOE by Jagadish et al. [31] (Table 6).

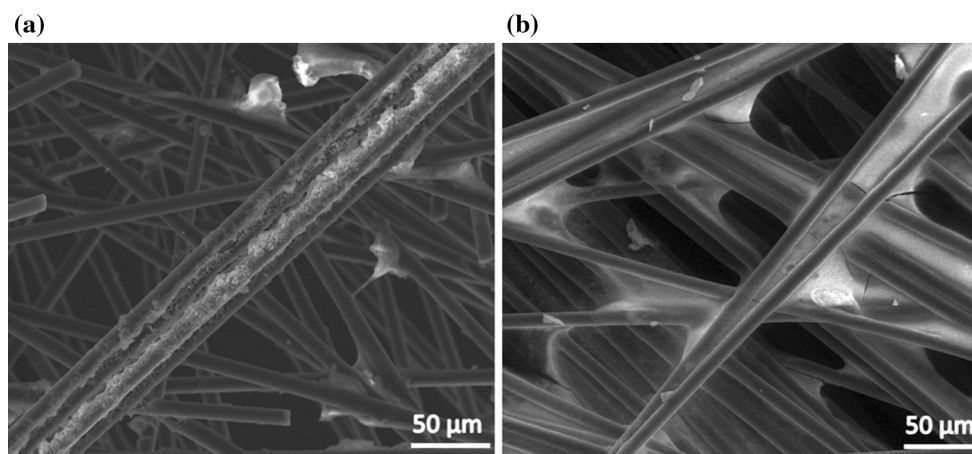


Figure 11 SEM images of **a** Bi₂Te₃-coated RCF (without DOE) [31]. **b** Bi₂Te₃-coated RCF (with DOE).

Moreover, a higher Seebeck coefficient was attained in this study despite using lower electrolyte concentration of 0.240 which is approximately 45% lesser than the electrolyte concentration used by Jagadish et al. [31]. In addition to that, this Seebeck coefficient was also attained at 50% less deposition time (0.5 h) than the 1-h deposition time. The high Seebeck coefficient is also complimented by the better Bi_2Te_3 coverage on RCF as shown in Fig. 11. It can be clearly observed from the SEM images that the RCF in Fig. 11b has a more uniform and widespread deposition of Bi_2Te_3 on its strands as compared to that of Fig. 11a that have site-specific Bi_2Te_3 deposited on certain areas of the fibre. Though the coverage of Bi_2Te_3 on RCF has improved, the coating was still not uniform throughout the strands of RCF to measure the coating thickness.

The increase in Seebeck coefficient in this study can be attributed to the contribution of the simultaneous interaction effects between deposition parameters that improved the overall deposition of Bi_2Te_3 on RCF. The previous study conducted by [31] only focused on single parameter variation at a time, namely the electrolyte concentration; however, this univariate approach as done by Jagadish et al. may not be able to predict the real process and interplay between the various parameters and thus unable to produce the global optimum response. A univariate approach does not take into consideration the individual effect of each deposition parameter and their combined interaction effects on the investigated response, hence missing an experimental domain that may have potentially resulted in higher optimum values.

Conclusion

The present work is one among the first to report the statistical evaluation of important deposition parameters for the electrodeposition of Bi_2Te_3 on RCF using design of experiments (DOE). Deposition potential, deposition time, deposition temperature and electrolyte composition were identified as vital process parameters that affect the Seebeck coefficient of Bi_2Te_3 . The optimum parameters obtained are deposition potential: -0.10 V, deposition time: 0.5 h, deposition temperature: 25 °C and electrolyte composition: 0.240 that yielded a decent Seebeck coefficient of -13.42 $\mu\text{V}/\text{K}$. The predicted and

experimental results were in close agreement with only 1.45% of difference, which indicates the robustness of the experimental design by DOE. Overall, it can be concluded that a multiparameter interaction yields a higher optimum response value than univariate experimental design due to the simultaneous effects of more than one deposition parameter as proven in this study.

Acknowledgements

The authors are grateful to the University of Nottingham, Malaysia campus, for its support in this research.

Compliance with ethical standards

Conflict of interest The authors declare that there is no conflict of interest regarding the publication of this article.

References

- [1] Sugiyama KI, Ueno H, Shiozaki M, Toriyama T, Sugiyama S (2005) Fabrication of flexible thermopile generator. *J Micromech Microeng* 15:S233. doi:[10.1088/0960-1317/15/9/S10](https://doi.org/10.1088/0960-1317/15/9/S10)
- [2] Kim SJ, We JH, Cho BJ (2014) A wearable thermoelectric generator fabricated on a glass fabric. *Energy Environ Sci* 7:1959. doi:[10.1039/c4ee00242c](https://doi.org/10.1039/c4ee00242c)
- [3] Kusagaya K, Takashiri M (2015) Investigation of the effects of compressive and tensile strain on n-type bismuth telluride and p-type antimony telluride nanocrystalline thin films for use in flexible thermoelectric generators. *J Alloys Compd* 653:480–485. doi:[10.1016/j.jallcom.2015.09.039](https://doi.org/10.1016/j.jallcom.2015.09.039)
- [4] Goncalves LM, Rocha JG, Couto C et al (2007) Fabrication of flexible thermoelectric microcoolers using planar thin-film technologies. *J Micromech Microeng* 17:S168–S173. doi:[10.1088/0960-1317/17/7/s14](https://doi.org/10.1088/0960-1317/17/7/s14)
- [5] Bubnova O, Khan ZU, Malti A et al (2011) Optimization of the thermoelectric figure of merit in the conducting polymer poly (3, 4-ethylenedioxythiophene). *Nat Mater* 10:429–433. doi:[10.1038/nmat3012](https://doi.org/10.1038/nmat3012)
- [6] Kim G-H, Shao L, Zhang K, Pipe KP (2013) Engineered doping of organic semiconductors for enhanced thermoelectric efficiency. *Nat Mater* 12:719–723. doi:[10.1038/nmat3635](https://doi.org/10.1038/nmat3635)
- [7] Jung KK, Jung Y, Choi CJ et al (2016) Flexible thermoelectric generator with polydimethyl siloxane in thermoelectric material and substrate. *Curr Appl Phys* 16:1442–1448. doi:[10.1016/j.cap.2016.08.010](https://doi.org/10.1016/j.cap.2016.08.010)

- [8] Goldsmid HJ, Douglas RW (1954) The use of semiconductors in thermoelectric refrigeration. *Br J Appl Phys* 5:458. doi:10.1088/0508-3443/5/12/513
- [9] Venkatasubramanian R, Siivola E, Colpitts T, O'quinn B (2001) Thin-film thermoelectric devices with high room-temperature figures of merit. *Nature* 413:597–602
- [10] Cholake ST, Moran G, Joe B et al (2016) Improved Mode I fracture resistance of CFRP composites by reinforcing epoxy matrix with recycled short milled carbon fibre. *Constr Build Mater* 111:399–407. doi:10.1016/j.conbuildmat.2016.02.039
- [11] Li M, Li S, Liu J et al (2016) Striking effect of epoxy resin on improving mechanical properties of poly(butylene terephthalate)/recycled carbon fibre composites. *Compos Sci Technol* 125:9–16. doi:10.1016/j.compscitech.2016.01.015
- [12] Feng N, Wang X, Wu D (2013) Surface modification of recycled carbon fiber and its reinforcement effect on nylon 6 composites: mechanical properties, morphology and crystallization behaviors. *Curr Appl Phys* 13:2038–2050. doi:10.1016/j.cap.2013.09.009
- [13] Wong KH, Pickering SJ, Rudd CD (2010) Recycled carbon fibre reinforced polymer composite for electromagnetic interference shielding. *Compos A Appl Sci Manuf* 41:693–702. doi:10.1016/j.compositesa.2010.01.012
- [14] Wang D, Su Y, Chen D et al (2014) Preparation and characterization of poly(3-octylthiophene)/carbon fiber thermoelectric composite materials. *Compos B Eng* 69:467–471. doi:10.1016/j.compositesb.2014.10.007
- [15] Tsukamoto J, Takahashi A, Tani T, Ishiguro T (1989) Thermoelectric power of heat-treated CVD carbon fibers. *Carbon* 27:919–923. doi:10.1016/0008-6223(89)90042-0
- [16] Hambach M, Möller H, Neumann T, Volkmer D (2016) Carbon fibre reinforced cement-based composites as smart floor heating materials. *Compos B Eng* 90:465–470. doi:10.1016/j.compositesb.2016.01.043
- [17] Ma Y, Johansson A, Ahlberg E, Palmqvist AEC (2010) A mechanistic study of electrodeposition of bismuth telluride on stainless steel substrates. *Electrochim Acta* 55:4610–4617. doi:10.1016/j.electacta.2010.03.018
- [18] Takahashi M (1993) Electrodeposition of Bi–Te alloy films. *J Electrochem Soc* 140:2550. doi:10.1149/1.2220860
- [19] Martín-González MS, Prieto AL, Gronsky R et al (2002) Insights into the Electrodeposition of Bi₂Te₃. *J Electrochem Soc* 149:C546. doi:10.1149/1.1509459
- [20] Magri P, Boulanger C, Lecuire J-M (1996) Synthesis, properties and performances of electrodeposited bismuth telluride films. *J Mater Chem* 6:773. doi:10.1039/jm9960600773
- [21] Miyazaki Y, Kajitani T (2001) Preparation of Bi₂Te₃ films by electrodeposition. *J Cryst Growth* 229:542–546
- [22] Qiu L, Zhou J, Cheng X, Ahuja R (2010) Electrochemical deposition of Bi₂Te₃-based thin films. *J Phys Chem Solids* 71:1131–1136. doi:10.1016/j.jpcs.2010.03.020
- [23] Wang W-LL, Wan C-CC, Wang Y-YY (2007) Composition-dependent characterization and optimal control of electrodeposited Bi₂Te₃ films for thermoelectric application. *Electrochim Acta* 52:6502–6508. doi:10.1016/j.electacta.2007.04.037
- [24] Kim MY, Oh TS (2009) Electrodeposition and thermoelectric characteristics of Bi₂Te₃ and Sb₂Te₃ films for thermopile sensor applications. *J Electron Mater* 38:1176–1181. doi:10.1007/s11664-008-0653-7
- [25] Yoo I-JJ, Myung NV, Lim DC et al (2013) Electrodeposition of Bi₂Te₃ thin films for thermoelectric application. *Thin Solid Films* 546:48–52. doi:10.1016/j.tsf.2013.05.036
- [26] Paunovic M, Schlesinger M (2006) *Fundamentals of electrochemical deposition*, 2nd edn. Wiley, Hoboken
- [27] Goux A, Pauport T, Chivot J, Lincot D (2005) Temperature effects on ZnO electrodeposition. *Appl Phys Lett* 50:2239–2248. doi:10.1016/j.electacta.2004.10.007
- [28] Rakhshani AE, Varghese J (1988) The effect of temperature on electrodeposition of cuprous oxide. *Phys Stat Sol* 105:183–188
- [29] Triefenbach F (2008) *Design of experiments: the D-optimal approach and its implementation as a computer algorithm*. Bachelor's Thesis in Information and Communication
- [30] Anderson MJ, Whitcomb PJ (2014) Practical aspects for designing statistically optimal experiments. *J Stat Sci Appl* 2:85–92
- [31] Jagadish PR, Li LP, Chan A, Khalid M (2016) Effect of annealing on virgin and recycled carbon fiber electrochemically deposited with N-type bismuth telluride and bismuth sulfide. *Mater Manuf Processes* 31:1223–1231. doi:10.1080/10426914.2015.1090590
- [32] Raissi S, Farsani R-E (2009) Statistical process optimization through multi-response surface methodology. *World Acad Sci Eng Technol* 51:267–271
- [33] Yoo BY, Huang C-K, Lim JR et al (2005) Electrochemically deposited thermoelectric n-type Bi₂Te₃ thin films. *Electrochim Acta* 50:4371–4377. doi:10.1016/j.electacta.2005.02.016
- [34] Pang EJX, Pickering SJ, Chan A et al (2012) N-type thermoelectric recycled carbon fibre sheet with electrochemically deposited Bi₂Te₃. *J Solid State Chem* 193:147–153. doi:10.1016/j.jssc.2012.04.046
- [35] Szymczak J, Legeai S, Michel S et al (2014) Electrodeposition of stoichiometric bismuth telluride Bi₂Te₃ using a piperidinium ionic liquid binary mixture. *Electrochim Acta* 137:586–594. doi:10.1016/j.electacta.2014.06.036

- [36] Kim D-H, Lee G-H (2006) Effect of rapid thermal annealing on thermoelectric properties of bismuth telluride films grown by co-sputtering. *Mater Sci Eng, B* 131:106–110. doi:[10.1016/j.mseb.2006.03.034](https://doi.org/10.1016/j.mseb.2006.03.034)
- [37] İbrahi Coşkun M, Karahan İH, Yücel Y (2014) Optimized electrodeposition concentrations for hydroxyapatite coatings on CoCrMo biomedical alloys by computational techniques. *Electrochim Acta* 150:46–54. doi:[10.1016/j.electacta.2014.10.120](https://doi.org/10.1016/j.electacta.2014.10.120)
- [38] Gautier P, Vallee A, Sinito C et al (2016) Diamond and related materials effect of growth temperature on the electrodeposition of zinc oxide layers on diamond surfaces. *Diam Relat Mater* 62:1–6. doi:[10.1016/j.diamond.2015.12.005](https://doi.org/10.1016/j.diamond.2015.12.005)
- [39] Sanchez S, Levy-Clement C, Ivanova V (2012) Electrochemical deposition of ZnO thin films and nanowires for photovoltaic applications. *J Electrochem Soc* 159:D705–D712. doi:[10.1149/2.024212jes](https://doi.org/10.1149/2.024212jes)
- [40] Zhu T, Chong MN, Phuan YW et al (2016) Effects of electrodeposition synthesis parameters on the photoactivity of nanostructured tungsten trioxide thin films: optimisation study using response surface methodology. *J Taiwan Inst Chem Eng* 61:196–204. doi:[10.1016/j.jtice.2015.12.010](https://doi.org/10.1016/j.jtice.2015.12.010)